

# An elastic, plastic, viscous model for slow shear of a liquid foam

P. Marmottant and F. Graner<sup>a</sup>

Laboratoire de Spectrométrie Physique, UMR5588 CNRS-Université Grenoble I, B.P. 87, F-38402 St Martin d'Hères Cedex, France

Received 10 October 2006 and Received in final form 7 January 2007

Published online: 13 August 2007 – © EDP Sciences / Società Italiana di Fisica / Springer-Verlag 2007

**Abstract.** We suggest a scalar model for deformation and flow of an amorphous material such as a foam or an emulsion. To describe elastic, plastic and viscous behaviours, we use three scalar variables: elastic deformation, plastic deformation rate and total deformation rate; and three material-specific parameters: shear modulus, yield deformation and viscosity. We obtain equations valid for different types of deformations and flows slower than the relaxation rate towards mechanical equilibrium. In particular, they are valid both in transient or steady flow regimes, even at large elastic deformation. We discuss why viscosity can be relevant even in this slow shear (often called “quasi-static”) limit. Predictions of the storage and loss moduli agree with the experimental literature, and explain with simple arguments the non-linear large amplitude trends.

**PACS.** 83.60.Df Nonlinear viscoelasticity – 83.60.La Viscoplasticity; yield stress – 83.80.Iz Emulsions and foams

## 1 Introduction

Elastic materials deform reversibly [1]; plastic materials can be sculpted, that is, they can be deformed into a new shape and keep it [2]; and viscous materials flow [3]. A wide variety of materials display a combination of these properties, such as elasto-plastic metals and rocks, visco-elastic polymer solutions or visco-plastic mineral suspensions [4–6].

Liquid foams, that is gas bubbles separated by liquid walls, are visco-elasto-plastic [7–9]: they are elastic at low strain, plastic at high strain and flow under high shear rate. This is also the case for other concentrated suspensions of deformable objects in a liquid [4,10,11], such as droplets in emulsions, vesicles suspensions, or red blood cells in blood.

Despite a large literature on experiments and simulations (see [9] for a review), we lack an unified theoretical description of foams. There is no consensus yet on a central question: what are the physically relevant variables? A series of statistical models focus on fluctuations and their correlations [12–16]. Conversely, recent contributions [17–23] focus on average macroscopic quantities to obtain a more classical continuous description.

Here we choose to group three macroscopic quantities which are measurable as averages on microscopical details [17]: i) Elastic deformation is a state variable [24] reversibly stored by the foam's microstructure, that is, the

shape of bubbles [25,26]; it determines the elastic contribution to the stress. ii) Plastic deformation results in energy dissipation analogous to solid friction. iii) Large-scale velocity gradients are associated with a viscous friction. Each of the three mechanical behaviors is associated with a material-specific parameter: elastic modulus, yield deformation and viscosity.

For simplicity, we assume here that these parameters are constant and the equations are linear. We consider here homogeneous deformation of a material, not depending on space coordinates. We consider only the magnitude of deformation, but not spatial orientation: the material state variables are all scalars. This represents an incompressible liquid foam, where the deformation is a pure shear. We assume that this shear is slow enough so that the foam is always close to mechanical equilibrium, but quick enough to neglect coarsening such as due to gas diffusion between bubbles, or bubble coalescence due to soap film breakage. Although this model is minimal, it is written with enough generality to enable for extensions to higher dimensions using tensors (the correspondance with tensors introduces a factor 1/2, see Sect. 4.3), to higher shear rates, and to other ingredients such as external forces (to be published).

This paper is organised as follows. Section 2 introduces a visco-elasto-plastic model (Eqs. (3,7)) based on two scalar variables: the elastic deformation and the (slow) shear rate (Fig. 3). The rate of plastic deformation is determined by both the applied shear rate, and the current state of the elastic deformation (or equivalently the elastic part of the stress) rather than by the total stress [27,28].

<sup>a</sup> e-mail: graner@ujf-grenoble.fr

Section 3 presents scalar predictions of creep and oscillatory responses. The storage and loss moduli predicted as a function of the strain amplitude agree with experimental data without any adjustable parameters, using only the three model-independent parameters determined by experiments (yield point, shear modulus, viscosity). The agreement becomes very good if we describe the plastic yielding as a gradual transition spreading between an onset value of deformation and a saturation value (Eq. (5)). Section 4 summarises and discusses our model, and opens some perspectives.

## 2 Model

### 2.1 Kinetics

#### 2.1.1 Elastic and plastic strain

The elastic deformation  $U$  is a *state variable*, that is an intrinsic property of the foam's current deformation state. We note its time derivative  $dU/dt$ . Conversely, we use a dot for the total strain rate  $\dot{\epsilon}$  and the plastic strain rate  $\dot{\epsilon}_P$ , emphasising that they are not the time derivative of a state variable. For instance, the time integral  $\epsilon = \int \dot{\epsilon} dt$  of the velocity gradient is the gradient of displacement (more generally, for large deformations, it is a function of the displacement): it is extrinsic and *explicitly depends* on the sample's past history.

The total applied deformation rate is shared between elastic deformation  $U$  and the plastic deformation rate:

$$\dot{\epsilon} = \frac{dU}{dt} + \dot{\epsilon}_P. \quad (1)$$

In the particular case of an elastic regime,  $\dot{\epsilon}_P = 0$ , the elastic deformation  $U$  is equal to the total applied deformation on the material  $\epsilon$ . Thus, in an elastic regime, no intrinsic definition of  $U$  is necessary.

However, as soon as  $\dot{\epsilon}_P \neq 0$ , the situation changes.  $U$  and  $\dot{\epsilon}$  become independent variables, and  $\epsilon = \int \dot{\epsilon} dt$  does not define the elastic deformation. In the extreme example of a steady flow,  $dU/dt = 0$ , then  $\dot{\epsilon} = \dot{\epsilon}_P$ :  $U$  and  $\dot{\epsilon}$  are no longer correlated.

These variables are macroscopic:  $U$  is related to the elastic contribution to macroscopic stress and  $\dot{\epsilon}_P$  to the irreversibility of the stress *versus* total strain curve. In the specific case of foams, they can be traced back to detailed properties of the bubbles pattern: independent, intrinsic definition [24] based on geometry (shape of bubbles [26]) for  $U$ ; and topological rearrangements called ‘‘T1 processes’’ [14, 29, 30] (using their rate and orientation [17]) for  $\dot{\epsilon}_P$ .

#### 2.1.2 Sharing the total strain

The problem now is to express how, in equation (1),  $\dot{\epsilon}$  is shared between  $dU/dt$  and  $\dot{\epsilon}_P$ . We must write a closure relation between these variables, for instance by expressing

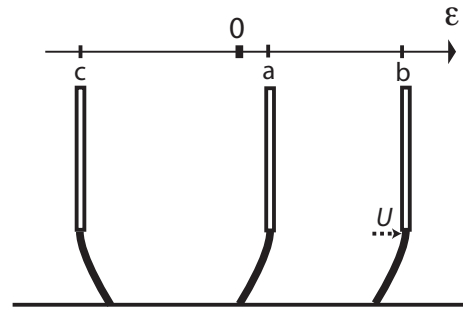


**Fig. 1.** Analog scalar system: an elastic brush whose flexion is  $U$  stick/slipping on wall. We represent several states, for an imposed oscillatory ‘‘painting-like’’ motion of the handle  $\epsilon$ , from rest position 0: (a) onset of sliding to the right, (b) far-right position, (c) far-left position.

how  $\dot{\epsilon}_P$  depends on the current state of elastic deformation and on the applied deformation rate:  $\dot{\epsilon}_P(U, \dot{\epsilon})$ . We use the following three hypotheses leading to equation (2).

First we describe an abrupt transition from elastic to plastic regime, as could be the case for an ordered foam [31]. To indicate that T1s appear when the absolute value of deformation  $|U|$  exceeds the yield deformation  $U_Y$ , we introduce the discontinuous Heaviside function  $\mathcal{H}$  (which is zero for negative numbers, and 1 for numbers greater than or equal to zero). This hypothesis can be relaxed in the Section 2.1.3, introducing a more progressive transition.

Secondly, we account for the hysteresis. Plastic rearrangements occur when the deformation rate  $\dot{\epsilon}$  and the current deformation  $U$  have the same sign, and again we express it using  $\mathcal{H}$ . Else, the deformation rate results in elastic unloading, and the deformation gets smaller than the yield deformation.

Thirdly, we use the fact that, in a slowly sheared motion, the only relevant time scale to fix the rate of plastic rearrangements is  $\dot{\epsilon}$ .

Eventually, the plasticity equation writes

$$\dot{\epsilon}_P = \mathcal{H}(|U| - U_Y) \mathcal{H}(U\dot{\epsilon}) \dot{\epsilon}. \quad (2)$$

Equation (2) can be used to close the system of equations. Injecting it in equation (1) yields an evolution equation of  $U$  as a function of the applied shear rate  $\dot{\epsilon}$ :

$$\frac{dU}{dt} = \dot{\epsilon} [1 - \mathcal{H}(|U| - U_Y) \mathcal{H}(U\dot{\epsilon})]. \quad (3)$$

In equation (3)  $U_Y$  appears as the stable value for  $U$ , that is, a fixed point, at least if  $\dot{\epsilon} > 0$ ; else, the stable fixed point is  $-U_Y$ .

To visualise the direction and the amplitude of the deformation  $U$ , we suggest an analogy with the motion of a brush on a wall (Fig. 1). The handle of the brush moves with an oscillatory position  $\epsilon$  parallel to the wall (analog of the imposed scalar deformation of the material), while the displacement of the handle with respect to the brush tip is  $U$  (the analog of the internal elasticity of the material). The sliding velocity of the contact point is therefore  $\dot{\epsilon}_P$  according to equation (1) and is the analog of plasticity in a material.

### 2.1.3 Gradual transition to plasticity

In a disordered foam, for instance with a wide distribution of bubble sizes, topological rearrangements do not necessarily occur for the same value of deformation.

We therefore distinguish two different yield deformations. First, a *plasticity yield*  $U_y$ , where deformation ceases to be reversible, as defined in material sciences. It is the highest deformation for which there is no T1. It is characteristic of the microstructure, and can even be close to zero for a very disordered foam.

Second, a *saturation yield*  $U_Y$ , the saturation value of elastic deformation at which the material can flow with arbitrary large total deformations (for instance in Bingham fluids). It is the lowest deformation for which the T1s convert the whole total strain into plastic strain. That is,  $U_Y$  is the collapse limit at which a material structure cannot sustain stress.

We interpolate between  $U_y$  and  $U_Y$  using a function  $h(U)$  which we call a *yield function*. It should be a growing (or at least non-decreasing) function of  $U$  for  $U > 0$ , and  $h(-U) = h(U)$ . Moreover,  $h(0) = 0$ , so that  $h(U) \geq 0$  for all  $U$ . Beside that, there is no special requirement on  $h$ , which even does not need to be continuous. Now,  $U_y$  is defined as the largest value of  $U$  for which  $h(U) = 0$ , and  $U_Y$  as the smallest value of  $U$  for which  $h(U) = 1$ . They do not necessarily correspond to any singularity in  $h$ . We show in appendix that the precise shape of  $h$  is unimportant: only  $U_y$  and  $U_Y$  determine the material's behaviour. However it is useful for theory to derive analytical equations.

The yield function  $h$  depends on the material under consideration, and can in principle be measured experimentally. By definition,  $h = 0$  corresponds to a purely elastic state where the elastic deformation follows the applied deformation. Conversely, for  $h = 1$  the plasticity rate is equal to the deformation rate. Such a smooth transition from elasticity to plasticity generalises the postulate (2) as

$$\dot{\epsilon}_P = h(U) \mathcal{H}(U\dot{\epsilon}) \dot{\epsilon}. \quad (4)$$

Note that we could in principle smoothen out the remaining Heaviside function too: depending on microscopical details, it could be conceivable that some T1s appear during the unloading. We do not explore this possibility here, because we seldom observe this effect and it does not seem to improve significantly the predictions presented below.

Injecting equation (4) into equation (1) we obtain

$$\frac{dU}{dt} = \dot{\epsilon} [1 - h(U) \mathcal{H}(U\dot{\epsilon})]. \quad (5)$$

Again, the fixed points are  $U = \pm U_Y$  according to the sign of  $\dot{\epsilon}$ .

## 2.2 Dynamics

### 2.2.1 Slow shear: foam close to equilibrium

In a foam, bubbles can swap neighbours giving rise to T1 topological rearrangements. A T1 is an infinitely

short event during which the energy is continuous. Thus it does not dissipate energy by itself, but it brings the foam to an out-of-equilibrium state. It is thus followed by a dissipation of energy during the relaxation towards another equilibrium configuration, with a microscopical relaxation time  $\tau_{\text{relax}}$ .

The average lifetime of a contact between two bubbles is  $f^{-1}$ , where  $f$  is the average frequency of T1s per bubble contact. If  $f\tau_{\text{relax}} \ll 1$ , the foam evolves (it is not static) but spends most of the time at or very close to mechanical equilibrium states. Thus Plateau rules of local mechanical equilibrium [8] are (almost) always satisfied, up to corrections of order  $f\tau_{\text{relax}}$ .

The frequency  $f$  can be determined by various causes of perturbations, for instance coarsening [8]. In rheology, it is determined by the plastic deformation rate  $\dot{\epsilon}_P$  [17]. For dimensional reasons,  $f$  is proportional to  $\dot{\epsilon}_P$ . Since the plasticity amplitude  $\dot{\epsilon}_P$  is always smaller than the deformation rate  $\dot{\epsilon}$  (see Eqs. (2) and (4)), the regime close to equilibrium is obtained in the slow shear limit:

$$\dot{\epsilon}\tau_{\text{relax}} \ll 1. \quad (6)$$

### 2.2.2 Contributions to total stress

We now include an additional viscous dissipation from the global deformation of the network of bubbles. This contribution is not linked to the relaxation of rearrangements, and does not modify the slow evolution of deformation.

We consider two separate contributions to stress, under the following hypotheses. According to experimental tests [26], we consider an elastic contribution to the stress  $\sigma^{\text{el}} = \mu U$  proportional to the elastic deformation  $U$ , where  $\mu$  is the shear elastic modulus. It describes a classical elastic behaviour, with a reversible restoring force.

According to the model proposed by Kraynik and co-workers [7, 32], we consider a viscous contribution to the stress due to large scale velocity gradients:  $\sigma^{\text{vis}} = \eta \dot{\epsilon}$ , where  $\eta$  is a macroscopic viscosity. It describes a classical fluid behaviour: the corresponding dissipated power is quadratic, proportional to  $\dot{\epsilon}^2$ .

In the spirit of a polymeric model [4], we assume that the stresses add up (Fig. 2):

$$\begin{aligned} \sigma &= \sigma^{\text{el}} + \sigma^{\text{vis}} \\ &= \mu U + \eta \dot{\epsilon}. \end{aligned} \quad (7)$$

The material is characterised by the coefficients  $\eta$ ,  $\mu$  and  $U_Y$  (and  $U_y$  in the case of gradual plasticity). Measuring experimentally, and understanding theoretically the physical origin of these coefficients, requires specific studies for each material considered: this is beyond the scope of the present paper. In principle, they can be rank-four tensors (anisotropic material). They can even vary with the material's state (non-linear material), for instance in a shear-thinning case.

As opposed to the crossover from elastic to plastic regimes, which is topological and is visible on images, here the crossover from the elastic to the fluid regime can be

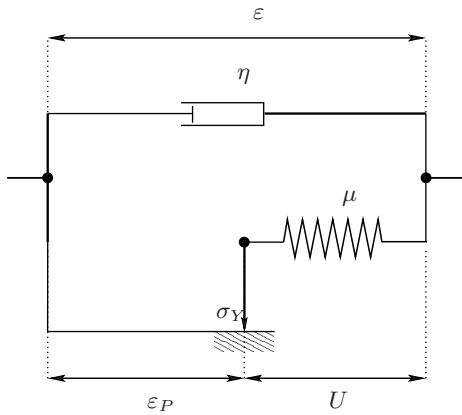


**Fig. 2.** A linear elasto-visco-plastic rheological model.

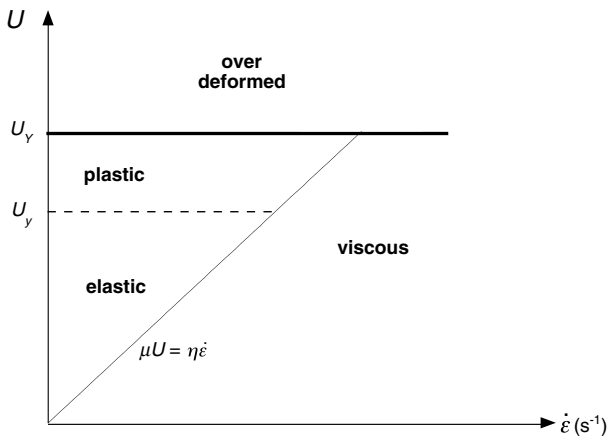


**Fig. 3.** Scalar phase diagram for a slowly sheared foam or an emulsion. Axes are experimentally measurable [17] local variables: shear rate  $\dot{\epsilon}$  and elastic deformation  $U$ . The crossover from elastic to plastic is defined as the onset of the first isolated topological rearrangements; it occurs around  $U_Y$ , with possible precursors around  $U_y$ . The yield deformation  $U_Y$  corresponds to a macroscopic rate of topological rearrangements. The crossover from solid to fluid is defined by the equality of viscous and elastic stresses. The slowly sheared regime presented here ceases to be valid when  $\dot{\epsilon}$  becomes comparable to  $\tau_{\text{relax}}^{-1}$ , inverse of the microscopical relaxation time.

detected only by measuring forces. It occurs when the viscous contribution to the stress becomes larger than the elastic one. Figure 3 thus plots the line corresponding to the crossover:  $\mu U = \eta \dot{\epsilon}$ .

Defining the macroscopic local Weissenberg number as

$$\text{Wi}_M \equiv \frac{\eta \dot{\epsilon}}{\mu}, \quad (8)$$

the crossover between elastic and fluid regime occurs at  $\text{Wi}_M = U$ .

Upon increasing  $\dot{\epsilon}$  from the plastic regime where  $U$  is close to  $U_Y$ , we predict a crossover from a stress bounded by a constant value  $\mu U_Y$  (with a dissipated power linear in  $\dot{\epsilon}$ , see next section) to a stress linear in  $\eta \dot{\epsilon}$  (with a dissipated power quadratic in  $\dot{\epsilon}$ ), characteristic of a viscous friction. The crossover from a plastic regime to a

fluid regime occurs when  $\eta \dot{\epsilon}$  is equal to  $\mu U_Y$ , *i.e.* when  $\text{Wi}_M = U_Y$ .

Since the plastic deformation is not bound, in the plastic regime the foam can flow indefinitely. As in hydrodynamics, the displacement field itself is no longer relevant. The plastic flow [5,6] and the viscous flow [3] look the same; their difference is not kinematic but dynamic: stresses are independent of and proportional to  $\dot{\epsilon}$ , respectively.

### 2.2.3 Dissipation

The close to equilibrium criterion (Eq. (6)) regards time scales, and is not a criterion based on the absence or presence of dissipation. Viscous dissipative effects can indeed be observed when considering measurements of the loss modulus at very low amplitude oscillations, and hence at very slow shear rate (as presented below in Figs. 9–11). In fact, dissipation is absolutely necessary to relax towards equilibrium: it damps oscillations and decreases the energy. Note that a “quasi-static” regime, that is a succession of equilibrium states, necessarily obeys the equilibrium criterion; but it is not sure that the reverse is true. In fact, reference [33] claims that in the slowly sheared Couette flow by [34] the velocity profile is determined by the ratio of velocity-dependent forces (internal viscosity and external friction on the plates of glass): static simulations are inappropriate.

As already mentioned, a T1 by itself, that is a side swapping, is an infinitesimally short topological event, during which the foam energy is continuous: there is no instantaneous dissipation. However, the T1 puts the foam in an out-of-equilibrium state. During a time  $\tau_{\text{relax}}$  the foam relaxes to a local energy minimum by dissipating an energy  $\delta E$ . A smaller microscopical dissipation yields a shorter relaxation time  $\tau_{\text{relax}}$ , and a larger *instantaneous* dissipated power, of order  $\mathcal{P}_{\text{diss}} = \delta E / \tau_{\text{relax}}$ . But the amount of energy dissipated,  $\delta E$ , is independent of the dissipation. Thus the dissipated power *averaged* over a long time (longer than  $\dot{\epsilon}^{-1}$ ) is of order

$$\langle \mathcal{P}_{\text{diss}} \rangle = f \delta E \sim \dot{\epsilon}_P \delta E \sim \dot{\epsilon} \delta E. \quad (9)$$

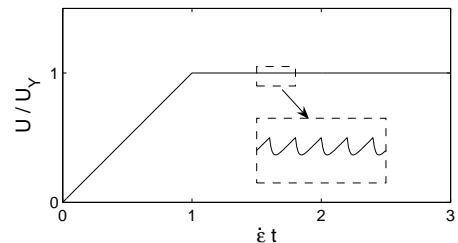


**Fig. 4.** Schematic impact of individual microscopic rearrangements on the stored elastic deformation  $U$ , for a constant loading rate  $\dot{\epsilon}$ . Rearrangements relax exponentially the deformation over a time  $\tau_{\text{relax}}$ , with here  $\dot{\epsilon} \tau_{\text{relax}} = 0.02 \ll 1$ . In the present macroscopic model, rearrangements are coarse-grained.

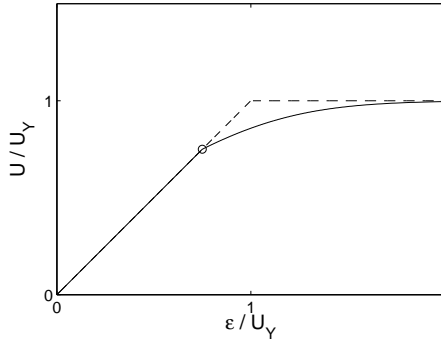


**Fig. 5.** Response to imposed shear for two examples of yield functions. Dashed solid line: abrupt transition,  $h(U) = \mathcal{H}(U - U_Y)$  (Eq. (2)). Thick line: finite  $U_y$ , and linear interpolation  $h(U) = (U - U_y)/(U_Y - U_y)\mathcal{H}(U - U_y)$  (Eq. (A.3)). Here  $U_y = 0.75 U_Y$ . See Figure 12 for more examples.

This dissipated power is proportional to  $\dot{\varepsilon}$ , and not quadratic as in viscous flows, although the microscopical origin is a local viscous dissipation [35].

The elastic deformation is almost independent on the shear rate  $\dot{\varepsilon}$  (see Fig. 4). To obtain a steady shear in a solid regime, when  $U$  saturates at the value  $U_Y$ , an experimentalist has to apply a constant external force which balances the average elastic stress, and does not depend on  $\dot{\varepsilon}$ .

Such a dissipated power linear in  $\dot{\varepsilon}$ , and a steady force which does not depend on  $\dot{\varepsilon}$ , are characteristic of a solid friction [36,37].

### 3 Prediction and tests

We model the foam response in one type of mechanical experiment, imposed deformation, and in two types of rheometrical experiments, creep flow and oscillating shear.

#### 3.1 Imposed shear

Here, we calculate the transient response during a shearing experiment, that is, the relation  $U(\varepsilon)$  between applied strain  $\varepsilon$  and elastic deformation  $U$ . For simplicity we take here  $\varepsilon = U = 0$  at the start of the experiment, but that assumption is easy to relax.

By direct integration, see appendix, we show the material's response: the elastic deformation  $U$  is close to the imposed strain  $\varepsilon$  at low applied strain, and tends to a saturation value at large applied strain. This robust behaviour does not depend much on the chosen yield function (see Fig. 5).

Thus the distribution of bubble sizes does not affect much the foam's transient response (as opposed to the liquid fraction, which drastically affects  $U_Y$  [31]). This explains why in the literature the function  $U(\varepsilon)$  is sometimes taken for simplicity as a piece-wise linear function or as a hyperbolic tangent [18].

This provides both the physical origin for the function  $\sigma(\varepsilon)$  of the model by Janiaud *et al.* [18], and a justification

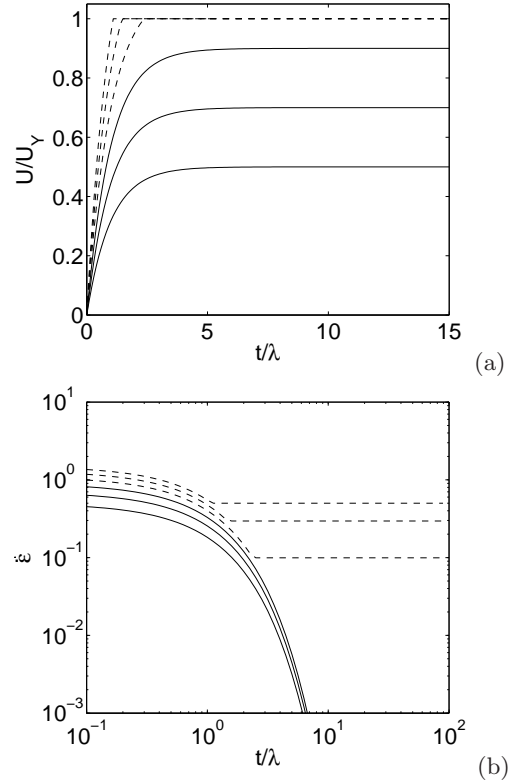


**Fig. 6.** Response to constant applied stress: (a) elastic deformation *versus* time and (b) local strain rate *versus* time, with a sharp transition to plasticity at  $U = U_Y$ . In both figures the stress grows from bottom to top: below yield values,  $\sigma_{\text{app}}$  equals to 0.5, 0.7, 0.9 times  $\sigma_Y$  (solid lines) and above yield values,  $\sigma_{\text{app}}$  equals to 1.1, 1.3, 1.5 times  $\mu U_Y$  (dashed lines). The time is adimensioned by  $\lambda = \eta/\mu$ .

for their (up to now arbitrary) expression  $\sigma = \sigma_Y f(\varepsilon/\varepsilon_Y)$ : the function  $f$  corresponds to the present elastic deformation  $U$ , while  $\varepsilon_Y$  is the yield deformation they chose equal to 1 for simplification.

#### 3.2 Creep under constant applied stress

A creep experiment in a rheometer applies a constant stress  $\sigma_{\text{app}}$ . It determines the effective viscosity  $\eta_{\text{eff}}$  from the steady shear rate:

$$\eta_{\text{eff}} = \lim_{t \rightarrow \infty} \frac{\sigma_{\text{app}}}{\dot{\varepsilon}(t)}. \quad (10)$$

The rheological response is found from equation (7) with  $\sigma = \sigma_{\text{app}}$ , and from equation (3). The elastic loading and the strain rate are plotted in Figure 6. The elastic deformation saturates to  $\sigma_{\text{app}}/\mu$  when it is below the threshold  $U_Y$ , and that it saturates to  $U_Y$  when above the threshold, over a characteristic time  $\lambda = \eta/\mu$ .

At long times, the strain rate tends towards vanishing values below yield stress (the flow stops), and tends to finite values above the yield:  $\dot{\varepsilon}(t \rightarrow \infty) = (\sigma_{\text{app}} - \mu U_Y)/\eta$ .

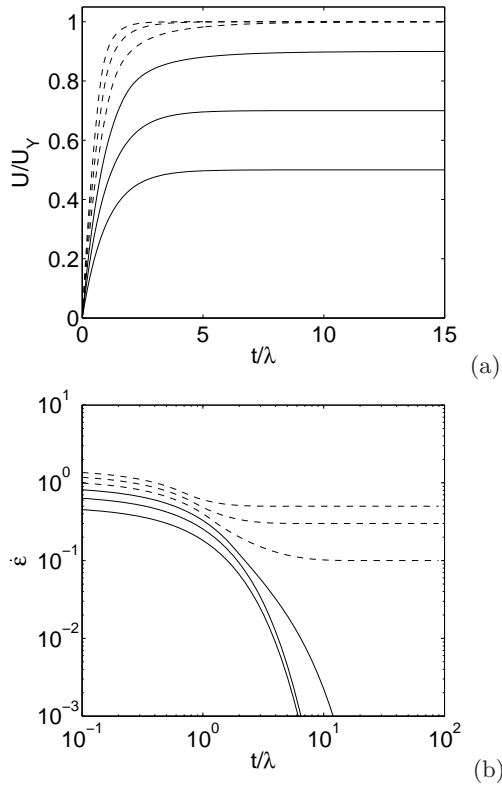


**Fig. 7.** Response to constant applied stress: (a) elastic deformation *versus* time and (b) strain rate *versus* time, with a smooth appearance of plasticity in between a plasticity onset threshold  $U_y$  and saturation  $U_Y$ . Plasticity starts at  $U_y = 0.75 U_Y$ , with the linear interpolation of equation (A.3). Same legend as previous figure.

We thus deduce the effective viscosity:

$$\eta_{\text{eff}} = \infty \quad \text{when} \quad \sigma_{\text{app}} \leq \mu U_Y, \quad (11)$$

$$\eta_{\text{eff}} = \frac{\eta}{1 - \frac{\mu U_Y}{\sigma_{\text{app}}}} \quad \text{when} \quad \sigma_{\text{app}} > \mu U_Y. \quad (12)$$

Taking a smooth plastic transition (Eq. (5)) does not change the overall features, except that the deceleration times below yield are no longer superimposed, see Figure 7.

### 3.3 Oscillating shear

A Couette apparatus is another typical rheometry experiment [9, 11, 29, 38]. It measures the stress  $\sigma(t)$  on the walls while imposing an applied sinusoidal shear strain of pulsation  $\omega = 2\pi/T$ :

$$\epsilon = \gamma \sin(\omega t). \quad (13)$$

#### 3.3.1 Hysteresis cycle and non-linear response

To test the effect of hysteresis of the model we calculate the response to such a periodic oscillatory shear bounded

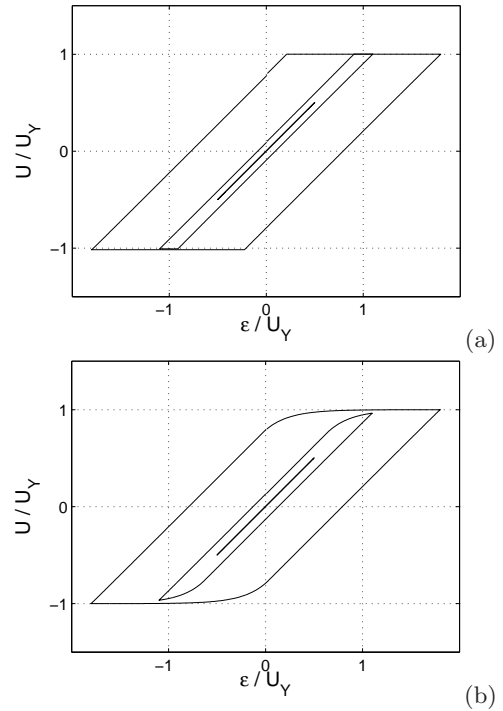


**Fig. 8.** Long-time periodic response to an oscillatory shear, for three amplitudes:  $\epsilon/U_Y = 0.75, 1.1$  and  $1.8$ . (a) In the case where the plasticity appears abruptly at  $U_Y$ , (b) gradual transition in between  $U_y$  and  $U_Y$ , with  $U_y/U_Y = 0.5$  (Eq. (A.3)).

by amplitudes  $\gamma$  and  $-\gamma$ . In the slow shear limit, the frequency does not play any explicit role. We can thus keep it fixed without loss of generality.

We integrate equation (3). The periodic elastic deformation-*versus*-strain curve is plotted in Figure 8, top. The stress response is linear in strain below the threshold, and saturates above in plastic regime, exhibiting a strong hysteresis.

Reversing the sign of the loading instantly stops any plasticity and the reponse becomes purely elastic. Multiple loading does not increase the slope of the loading part, nor the value of saturation yield; the foam is described as perfectly plastic. Such features are observed in experiments on other amorphous solids [39, 40] (as opposed to strain-hardening features of crystalline metals [2]).

Integration of equation (4) describes a smooth variation of deformation, see Figure 8, bottom.

#### 3.3.2 Storage and loss moduli: predictions

In complex notation the stress response  $\sigma^*$  is linked to the strain  $\epsilon^*$  by  $\sigma^* = (G' + iG'')\epsilon^*$ . Here  $G'$  is the storage modulus and  $G''$  the loss modulus of the material, defined as the in-phase and out-phase part of the response (first term in a Fourier series, see non-linear models [19, 41, 42]).

When increasing the amplitude  $\gamma$  of the imposed sinusoidal shear strain, the response is first linear until the amplitude at which  $G'$  and  $G''$  start to vary. In both the linear and non-linear regimes, the storage and loss moduli

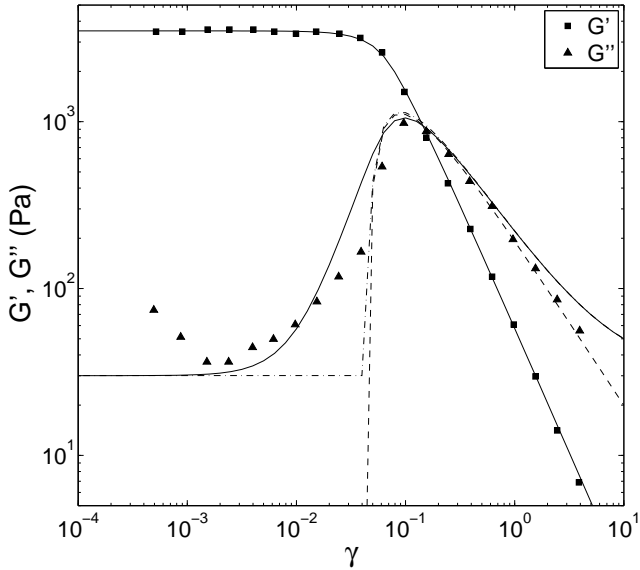


**Fig. 9.** Storage and loss moduli *versus* strain amplitude for a monodisperse emulsion. Symbols: experimental  $G'$  (circles) and  $G''$  (triangles) in a close-packed emulsion (Fig. 1 of Ref. [43], fraction of the continuous phase 20%, droplet size  $0.53\ \mu\text{m}$ , oscillation pulsation  $\omega = 1\ \text{rad s}^{-1}$ ). Lines: models for  $G'$  (solid line), and for  $G''$  with an abrupt transition (dashed line), with viscosity (dash-dotted line), with viscosity and a smooth yield function  $h = (U/U_Y)^2$ ,  $U_y = 0$  (solid line). Model parameters: shear modulus  $\mu = 1.7 \cdot 10^3\ \text{Pa}$ , yield deformation  $U_Y = 0.045$ , viscosity  $\eta = 30\ \text{Pa.s}$ .

are calculated as:

$$\begin{aligned} G' &= -\frac{1}{\gamma^2} \frac{1}{\pi\omega} \int_0^T \sigma(t) d\dot{\varepsilon}, \\ G'' &= \frac{1}{\gamma^2} \frac{1}{\pi} \int_0^T \sigma(t) d\varepsilon, \end{aligned} \quad (14)$$

$G'$  is proportional to the area enclosed by the  $(\sigma(t), \dot{\varepsilon}(t))$  curve, while  $G''$  is proportional to the area enclosed by the  $(\sigma(t), \varepsilon(t))$  curve. When plasticity occurs, the cycle has a non-vanishing area in the  $(\sigma(t), \varepsilon(t))$  diagram, meaning a non-vanishing loss modulus  $G''$ .

In the present model  $\sigma(t)$  depends on the current elastic deformation  $U(t)$  and shear rate  $\dot{\varepsilon}(t)$  (Eq. (7)). For the case of the abrupt elastic/plastic transition, the analytical integration of areas is simple and provides the following solutions for the moduli. Using equations (14) we obtain, when  $\gamma \ll U_Y$ :

$$\begin{aligned} G' &\simeq \mu, \\ G'' &= \eta, \end{aligned} \quad (15)$$

which is the usual linear visco-elastic regime. Note that our model predicts frequency-independant moduli, for a fixed small amplitude  $\gamma$ . At large amplitudes, when  $\gamma \gg U_Y$ :

$$\begin{aligned} G' &\simeq \mu \frac{4}{\pi} \left( \frac{U_Y}{\gamma} \right)^{3/2}, \\ G'' &= \mu \frac{4U_Y}{\pi\gamma} + \eta. \end{aligned} \quad (16)$$

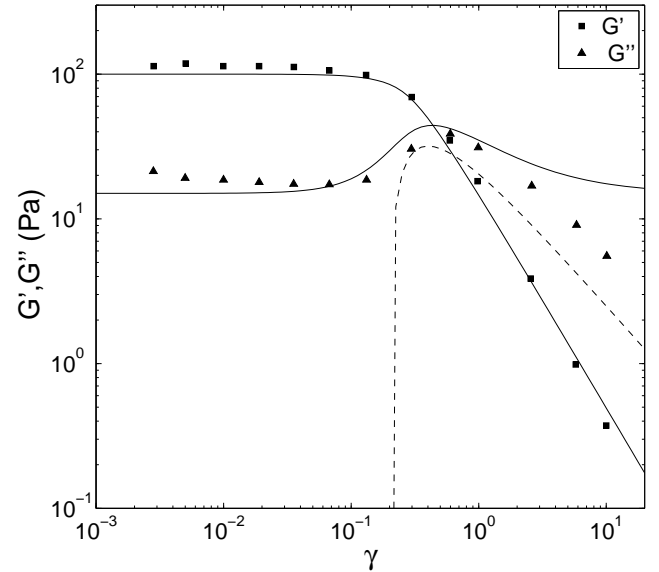


**Fig. 10.** Same as Figure 9 for a polydisperse foam [44]. Liquid fraction 5%, bubble size 40 to  $70\ \mu\text{m}$ ,  $\omega = 1\ \text{rad s}^{-1}$ . Lines: models for  $G'$  (solid line), and for  $G''$  with an abrupt transition (dashed line), with viscosity and a smooth yield function  $h = (U/U_Y)^2$ ,  $U_y = 0$  (solid line). Model parameters:  $\mu = 100\ \text{Pa}$ ,  $U_Y = 0.2$ ,  $\eta = 15\ \text{Pa.s}$ .

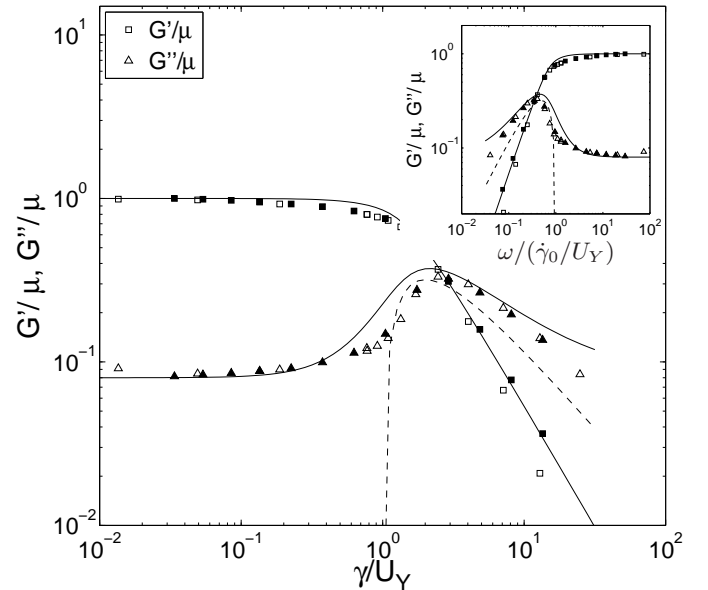


**Fig. 11.** Same as Figure 9 for a monodisperse foam [38]. Liquid fraction 8%, bubble size  $21\ \mu\text{m}$ ,  $\omega = 1\ \text{rad s}^{-1}$ . Data of  $G'$  and  $G''$  are normalised by  $\mu$  and  $\gamma$  by  $U_Y$ , while  $\eta\omega/\mu = 0.08$ . Same legend as Figure 10. Inset: strain-rate frequency superposition: same data plotted as a function of pulsation  $\omega$ , for a given maximum strain rate  $\dot{\gamma}_0 = \omega\gamma$  [20].

These asymptotic dependencies in  $\gamma^{-3/2}$  and  $\gamma^{-1}$ , respectively, are obtained analytically and are robust with respect to the model. The analytical expression of  $G'$  and  $G''$  over the whole range of  $\gamma$ , but with  $\eta = 0$  is explicitly presented in references [21, 22].

For a smooth yield function  $h$ , predictions are obtained numerically and plotted on Figures 9–11.

### 3.3.3 Comparison with experiments on emulsions and foams

Rheometry measurements of monodisperse emulsions [43] (Fig. 9) and polydisperse foams [38,44] (Figs. 10 and 11) directly yield, without hypotheses, the values of the material parameters required by the model. The shear modulus  $\mu$  is read from the value of  $G'$  at low amplitude. The viscosity  $\eta$  is read from the value of  $G''$  at low amplitude (or the value of the minimum, in Fig. 9, where the two data points at  $\gamma < 10^{-3}$  have too large error bars to be taken into account, according to T. Mason, private communication). The yield deformation  $U_Y$  is read from the intersection of low amplitude plateau of  $G'$  and its large amplitude  $-3/2$  exponent power law.

A purely elasto-plastic model is enough to predict  $G'$  correctly, over the whole range of amplitude, including the  $-3/2$  exponent power law. This simplest model also describes correctly the large amplitude trend for  $G''$ .

The low amplitude value of  $G''$  can be modelled by including a viscosity (dash-dotted line of Fig. 9), which confirms that viscosity is relevant even in such slowly sheared models. This procedure is at the expense of a slight over-prediction at large amplitudes. This latter aspect suggests a possible shear-thinning, that is a decrease of the viscosity  $\eta$  with the shear rate, similarly to the observed reduction of the drag of foams in motion in channels [31].

The agreement between the data and the model, without adjustable parameter, is good. It is still improved, even for  $G''$  at intermediate amplitudes, if we account for the fact that the first T1s appear gradually at a value  $U_y$  lower than  $U_Y$  (solid lines in figures for  $G''$ ). Even the value of  $U_y$  itself is not very important, and in order to avoid introducing a free parameter we use here  $U_y = 0$  and a smooth yield function.

These results suggest that data can be rescaled with the yield deformation  $U_Y$ , and it suggests a rescaling when plotting data as a function of frequency, following the strain-rate frequency superposition method (SRFS [20]). This method considers measurements with a fixed maximum strain rate  $\dot{\gamma}_0 = \omega\gamma$ , it is therefore equivalent to vary frequency or oscillation amplitude. The natural rescaling for pulsation that appears is  $\omega/b(\dot{\gamma}_0) = \omega/(\dot{\gamma}_0/U_Y) = U_Y/\gamma$ , see inset of Figure 11, and our model predicts the global shapes of the moduli curves as observed in [20]. The characteristic frequency  $b(\dot{\gamma}_0)$  is here linear in  $\dot{\gamma}_0$ , also in agreement with the trend observed in [20] for large enough strain rates.

## 4 Discussion

### 4.1 Discussion of the predictions

Independently from us, Höhler *et al.* solve a purely elasto-plastic model [21,22]. Since they neglect the viscosity, they can eliminate  $U$  and replace it by  $\sigma/\mu$ . The agreement of their model with data of Figure 11, as well as other experimental data, is good for  $G'$  over the whole range of amplitude; and also for  $G''$  but only at large amplitude,

where the dissipation comes from the relaxation after T1s rather than from  $\eta$ .

Our model describes better: i)  $G''$  at low amplitude using viscosity; and ii)  $G''$  at intermediate amplitudes, if we account for the fact that the first T1s appear at a value  $U_y$  lower than  $U_Y$ .

The predicted curves are robust with respect to  $U_y$ . This implies that we do not need to fit it; but that, conversely, we are not yet able to deduce  $U_y$  from  $G''$  data. If we had a direct experimental measurement of  $U_y$ , we could inject it in the model to predict  $G''$  at intermediate amplitudes, near  $U_Y$ , but the resulting predictions would be very similar to the present ones.

While  $U_y$  corresponds to the onset of isolated plastic events, at a deformation  $U_Y$  the plastic events have a macroscopic effect: they catch the total strain; the foam flows without increasing its deformation any longer.

The effective viscosity  $\eta_{\text{eff}}$  diverges to infinite values when  $\sigma_{\text{app}}/\mu \rightarrow U_Y^+$ . This means that the foam comes close to its yield deformation, in the fluid sense. This change in behaviour was shown by [45], and modelled by a granular model with a velocity-dependent friction. Here, the dynamics is entirely driven by a constitutive equation with shear-rate-independent parameters. It is the transient elastic loading that drives a transient flow, which stops when the stress is not strong enough.

The trends of Figure 6 agree with experimental data on various material reported in [45], at least with granular materials and emulsion. The present model does not predict the apparent shear-thinning behaviour observed with their experimental data with foams [45], where an increase of shear rate with time is found [46]. The low amplitude predictions for the visco-elastic regime (see Eq. (15)) are frequency-independent moduli. The limitation of the present model is thus that it does not fully capture the slight increase of the loss moduli at low frequency, and the  $\omega^{1/2}$  trend at large frequencies (see for instance the case of foams [9]).

### 4.2 Elastic, plastic, viscous model

A complete model for an elastic, plastic, viscous foam requires to recognise the role of three physical variables  $U$ ,  $\dot{\epsilon}$ ,  $\dot{\epsilon}_P$ . There is a relation between them (Eq. (1)). Unless specific approximations apply, a foam's representative volume element (RVE) is characterised by two independent variables: we suggest to select the local elastic deformation  $U$ , and the local shear rate  $\dot{\epsilon}$ , which are intuitive and physically relevant. Both of course depend on the sample's past history, but this history plays no explicit role. Both are always defined, whether in elastic, plastic or viscous regime [25]. Two recent works [20,47] find that  $G'$  and  $G''$  depend on the strain amplitude and on the strain rate (rather than on the frequency), in the same spirit as our phase diagram (Fig. 3).

Each volume element can thus be plotted as a point in a phase diagram (Fig. 3); that is, the  $(\dot{\epsilon}, U)$ -plane [15]. In a heterogeneous flow, different volume elements of the same foam are plotted as different points. A volume element's

evolution is a trajectory on this plane. *Simple* materials correspond to the axes of the plane: pure elastic and pure plastic regimes on the vertical axis, pure viscous regime (Navier-Stokes) on the horizontal axis.

The importance of  $U$  is the most original feature of the present model:  $U$  cannot be entirely determined by  $\dot{\varepsilon}$  since the latter can change sign;  $U$  cannot be entirely determined by  $\sigma$  if the viscous contribution is not negligible.

The yield function describing the occurrence of plasticity can be linked to the traditional hardening modulus, used for the description of plastic materials [48]. It is defined as  $K = d\sigma/d\varepsilon_p$ , while the elastic modulus is  $\mu = d\sigma/U$ . In the present model, the hardening modulus is dependent on the elastic deformation:  $K = 1/h(U) - 1$ . It therefore vanishes when  $U$  tends to its saturation value  $U_Y$ : at this point the material does not harden any more.

A deformation beyond  $U_Y$  is not accessible when starting from rest (Fig. 3). But the foam could initially be prepared (for instance artificially [49]) in a configuration very far from equilibrium. Under a steady shear rate  $\dot{\varepsilon}$ , the deformation  $U$  always tends towards  $U_Y(\dot{\varepsilon})$ , whether from below or from above.

In a flowing foam, there is always a viscous dissipation. Its contribution becomes dominant in front of the plastic dissipation if  $\dot{\varepsilon} > \mu U/\eta$ . This is compatible with the slow shear criterion,  $\dot{\varepsilon} \ll \tau_{\text{relax}}^{-1}$  (*i.e.* on a second Weissenberg number that is here  $\text{Wi}_m = \dot{\varepsilon}\tau_{\text{relax}} \ll 1$ ), if there is a scale separation between the microscopic relaxation time  $\tau_{\text{relax}}$  towards local equilibrium and the large scale time  $\eta/\mu$ . The dimensionless ratio  $\mu\tau_{\text{relax}}/\eta$  of microscopic to macroscopic times is analogous to the parameter  $I$  of granular materials [50].

### 4.3 Perspectives

This model could in principle be generalised to higher velocity gradients [23]. This would require a high flow velocity varying over a small scale, and  $\tau_{\text{relax}}$  could play an explicit role. The deviation from equilibrium, of order  $\dot{\varepsilon}\tau_{\text{relax}}$ , would become significant: for instance, under a steady shear the limit value of  $U$  could become larger than  $U_Y$ .

A rheometer such as a Couette apparatus can measure  $\sigma_{12} = \sigma$  (tangential force per unit wall surface) and  $\varepsilon_{12} = \varepsilon/2$  (components of the symmetrized deformation gradient), in a coordinate system aligned with walls. For comparison with tensorial data it is especially important to bear in mind that there is a *factor* 1/2: the threshold  $U_Y$  on oscillation amplitude  $\varepsilon$  as measured by a Couette rheometer, corresponds to a threshold  $U_Y/2$  on the tensorial deformation  $\varepsilon_{12}$ . The present scalar approach can be generalised to take into account such an influence of the orientation of material deformation, as well as spatial variations [17, 51].

The present paper is a contribution to a lively debate. Can a foam be described as a continuous material? We tend here to answer “yes”, in the same spirit as many recent papers which describe or predict rheological properties at large scale [17, 18, 21–23, 26, 52]. Statistical descrip-

tions of fluctuations and their correlations [12, 13, 15, 16, 45] are then useful in describing even more complex rheological behaviour such as shear banding [14] or growing correlation length scale near the glass transition [53]. Interestingly, even in granular materials, where very large scale fluctuations are known to occur, a recent paper emphasises the dominant role of the “continuous material” description based on averages [50].

We thank E. Janiaud for critical reading of the manuscript, R. Höhler for comparison of our calculations before publication, F. Rouyer for providing experimental data, S. Ataei Talebi, I. Cheddadi, B. Dollet, C. Quilliet, C. Raufaste, and P. Saramito for discussions, T. Mason and A. Saint-Jalmes for comments on their experimental data.

## Appendix A. Elastic-plastic transition

### Appendix A.1. Transient response from rest

We assume (in this section only) that *the deformation rate  $\dot{\varepsilon}$  keeps a constant sign*. Under this essential assumption, we can calculate analytically the transient response during a shearing experiment. That is, the relation  $U(\varepsilon)$  between applied strain  $\varepsilon = \int \dot{\varepsilon} dt$  and elastic deformation  $U$ .

The yield function  $h$  is defined to interpolate between  $h(U) = 0$  for  $0 < U < U_y$ , and  $h(U_Y) = 1$ . By direct integration, equation (5) yields

$$\varepsilon = \int_0^U \frac{dU}{1 - h(U)}. \quad (\text{A.1})$$

Here, without further loss of generality, we have also assumed (but it is easy to relax) that  $\varepsilon = U = 0$  at the start of the experiment, and that  $\dot{\varepsilon} \geq 0$ , so that  $U \geq 0$  too.

Equation (A.1) yields the function  $\varepsilon(U)$ , which can be inverted to obtain  $U(\varepsilon)$ . These functions can be measured on experiments and compared with predictions derived from direct measurements of  $h(U)$ .

Whatever the function  $h(U)$ , equation (A.1) implies that  $U \approx \varepsilon$  as long as  $U < U_y$ : applied and elastic deformation are equal in the elastic regime. At the onset of plasticity (or topological changes),  $U > U_y$ , they differ. When  $U$  gets close to  $U_Y$  the r.h.s. of equation (A.1) diverges. Thus, when  $\varepsilon$  increases arbitrarily,  $U$  tends asymptotically towards the saturation value  $U_Y$ .

### Appendix A.2. Examples of yield functions $h$

Table 1 proposes a few examples of yield functions  $h$ , and some are plotted in Figure 12.

Equation (3) is only a particular case of the more general equation (5), with  $h$  being the discontinuous Heaviside function:

$$h(U) = \mathcal{H}(U - U_Y). \quad (\text{A.2})$$

Equation (A.1) thus includes the case of the abrupt transition.

**Table 1.** Elastic deformation for different examples of yield function  $h$ , for a non-deformed initial condition  $U(0) = 0$  and with  $\dot{\varepsilon}$  of constant sign.

Yield function $h$	Elastic response $U(\varepsilon)/U_Y$
$\mathcal{H}(U - U_Y)$	$\varepsilon - \mathcal{H}(\varepsilon/U_Y - 1)\varepsilon$
finite $U_y$ (Eq. (A.3))	equation (A.4)
$(U/U_Y)^0$	0
$(U/U_Y)^1$	$1 - \exp(-\varepsilon/U_Y)$
$(U/U_Y)^2$	$\tanh(\varepsilon/U_Y)$
$\sin^2(U/U_Y)$	$\arctan(\varepsilon/U_Y)$

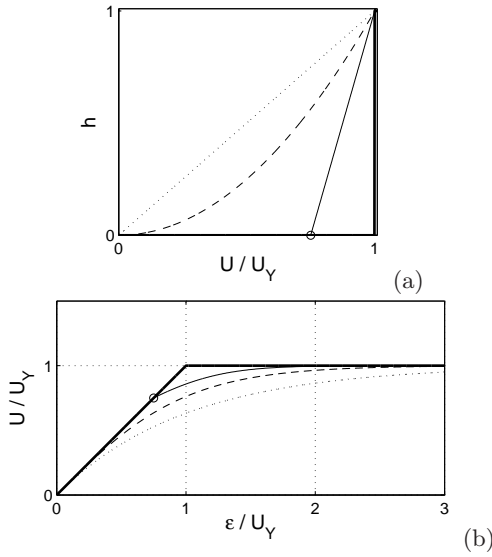


**Fig. 12.** Responses from rest for some examples of yield functions in Table 1. (a)  $h(U)$ ; (b)  $U/U_Y$  versus  $\varepsilon/U_Y$ : since they are very similar, for clarity only some of them are plotted. Thick solid line: abrupt transition,  $h(U) = \mathcal{H}(U - U_Y)$ . Thin line: finite  $U_y$ , here  $U_y = 0.75 U_Y$ , and linear interpolation  $h(U) = (U - U_y)/(U_Y - U_y)\mathcal{H}(U - U_y)$  (Eq. (A.3)). Dashes: vanishing  $U_y$  and quadratic interpolation,  $h = (U/U_Y)^2$ . Dots: vanishing  $U_y$  and linear interpolation,  $h = (U/U_Y)$ .

An example of a yield function with finite  $U_y$  is a piecewise linear function:

$$\begin{aligned} U \leq U_y & \quad h(U) = 0, \\ U \geq U_y & \quad h(U) = \frac{U - U_y}{U_Y - U_y}. \end{aligned} \quad (\text{A.3})$$

and equation (A.1) yields directly:

$$\begin{aligned} \varepsilon \leq U_y & \quad U(\varepsilon) = \varepsilon, \\ \varepsilon \geq U_y & \quad U(\varepsilon) = \frac{U_Y}{U_Y - U_y} \\ & \quad - \left( \frac{U_Y}{U_Y - U_y} - U_y \right) e^{-\left(\frac{\varepsilon - U_y}{U_Y - U_y}\right)}. \end{aligned} \quad (\text{A.4})$$

We can interpolate between abrupt and smooth transitions, using the family of model power law yield functions

$$h(U) = \left( \frac{U}{U_Y} \right)^n. \quad (\text{A.5})$$

For instance, the quadratic expression  $h(U) = (U/U_Y)^2$  yields  $U(\varepsilon) = U_Y \tanh(\varepsilon/U_Y)$ . With these functions, plasticity appears more or less gradually, as soon as  $U > 0$ . That is,  $U_y = 0$ . The limit  $n \rightarrow \infty$  is the Heaviside function (Eq. (A.2)).

More generally, the yield function can be thought as the convolution of the Heaviside function  $\mathcal{H}$  and a distribution of yield values  $p_Y$ :

$$h(U) = \int p_Y(U_Y) \mathcal{H}(|U| - U_Y) dU_Y. \quad (\text{A.6})$$

For instance, if the distribution of yield values  $p$  is a Dirac peak at  $U_Y$ , it results in a Heaviside yield function  $h$  (Eq. (A.2)).

### Appendix A.3. Robustness with respect to the choice of $h$

Some functions  $U(\varepsilon)$  from Table 1 are plotted in Figure 12b. Strikingly, they do not depend much on the actual expression of  $h(U)$ . In fact, only the expression of  $h$  near  $U_Y$  matters; the relation between  $\varepsilon$  and  $U$  is robust. The elastic deformation  $U$  is close to the imposed strain  $\varepsilon$  at low applied strain, and tends to a saturation value at large applied strain.

The only important feature of  $h$  is its derivative  $h'$  just below the yield point:

$$h' = \left( \frac{dh(U)}{dU} \right)_{U \rightarrow U_Y^-}. \quad (\text{A.7})$$

It determines how the fraction in the r.h.s. of equation (A.1) diverges. Thus  $U(\varepsilon)$  is not the same if  $h'$  is zero or infinite, or even not defined as in equation (A.2). If it is infinite,  $U$  reaches the saturation value at a finite value of applied deformation.

Conversely, if  $h'$  is finite, as in most examples of Table 1, the behaviour is universal. In equation (A.1), the fraction diverges as  $(U_Y - U)h'$ . Thus, whatever the value of  $h'$ ,  $\varepsilon(U)$  diverges logarithmically and  $U(\varepsilon)$  tends exponentially towards  $U_Y$ .

## References

1. L.D. Landau, E.M. Lifchitz, *Theory of Elasticity* (Reed, 1986).
2. J. Chakrabarty, *Theory of Plasticity* (McGraw-Hill Book Company, New York, 1978).
3. G.K. Batchelor, *An Introduction to Fluid Dynamics* (Cambridge University Press, Cambridge, 2000).
4. C.W. Macosko, *Rheology: Principles, Measurements and Applications* (Wiley-VCH, 1994).

5. D. François, A. Pineau, A. Zaoui, *Comportement mécanique des matériaux: viscosité, endommagement, mécanique de la rupture, mécanique du contact* (Hermès, 1993).
6. D. François, A. Pineau, A. Zaoui, *Comportement mécanique des matériaux: élasticité et plasticité* (Hermès, 1995).
7. A.M. Kraynik, *Annu. Rev. Fluid Mech.* **20**, 325 (1988).
8. D. Weaire, S. Hutzler, *The Physics of Foams* (Oxford University Press, Oxford, 1999).
9. R. Höhler, S. Cohen-Addad, *J. Phys.: Condens. Matter* **17**, R1041 (2005).
10. R.G. Larson, *The Structure and Rheology of Complex Fluids* (Oxford University Press, 1999).
11. T.G. Mason, J. Bibette, D.A. Weitz, *J. Colloid Interface Sci.* **179**, 439 (1996).
12. P. Sollich, F. Lequeux, P. Hebraud, M.E. Cates, *Phys. Rev. Lett.* **78**, 2020 (1997).
13. M.L. Falk, J.S. Langer, *Phys. Rev. E* **57**, 7192 (1998).
14. A. Kabla, G. Debrégeas, *Phys. Rev. Lett.* **90**, 258303 (2003).
15. G. Picard, A. Ajdari, F. Lequeux, L. Bocquet, *Phys. Rev. E* **71**, 010501 (2005).
16. P. Coussot, *Phys. Rev. Lett.* **95**, 078303 (2005).
17. P. Marmottant, B. Dollet, C. Raufaste, F. Graner, cond-mat/0609188.
18. E. Janiaud, D. Weaire, S. Hutzler, *Phys. Rev. Lett.* **97**, 038302 (2006).
19. K. Miyazaki, H.M. Wyss, D.A. Weitz, D.R. Reichman, *Europhys. Lett.* **75**, 915 (2006).
20. H.M. Wyss, K. Miyazaki, J. Mattsson, Z. Hu, D.R. Reichman, D.A. Weitz, *Phys. Rev. Lett.* **98**, 238303 (2007).
21. V. Labiausse, PhD Thesis, Université de Marne-la-Vallée (2004).
22. R. Höhler, S. Cohen-Addad, V. Labiausse, cond-mat/0610279.
23. P. Saramito, *J. Non-Newtonian Fluid Mech.* **145**, 1 (2007).
24. G. Porte, J.-F. Berret, J. Harden, *J. Phys. II* **7**, 459 (1997).
25. M. Aubouy, Y. Jiang, J.A. Glazier, F. Graner, *Granular Matter* **5**, 67 (2003).
26. M. Asipauskas, M. Aubouy, J.A. Glazier, F. Graner, Y. Jiang, *Granular Matter* **5**, 71 (2003).
27. N. Cristescu, I. Siliciu, *Viscoplasticity* (Martinus Nijhoff, 1982).
28. A.K. Miller, *Unified Constitutive Equations for Creep and Plasticity* (Elsevier Applied Science, 1987).
29. J. Lauridsen, M. Twardos, M. Dennin, *Phys. Rev. Lett.* **89**, 098303 (2002).
30. A.D. Gopal, D.J. Durian, *Phys. Rev. Lett.* **91**, 188303 (2003).
31. H.M. Princen, *J. Colloid Interface Sci.* **91**, 160 (1983).
32. A.M. Kraynik, M.G. Hansen, *J. Rheol.* **31**, 175 (1987).
33. E. Janiaud, D. Weaire, S. Hutzler, *Phys. Rev. Lett.* **93**, 18303 (2006).
34. G. Debrégeas, H. Tabuteau, J.-M. di Meglio, *Phys. Rev. Lett.* **87**, 178305 (2001).
35. G. Puglisi, L. Truskinovsky, *J. Mech. Phys. Solids* **53**, 655 (2005).
36. C.A. Coulomb, *Mémoires de l'Académie des Sciences (Paris)* (1779).
37. T. Baumberger, P. Berthoud, C. Caroli, *Phys. Rev. B* **60**, 3928 (1999).
38. F. Rouyer, S. Cohen-Addad, R. Höhler, *Colloid Surf. A* **263**, 111 (2005).
39. M. Aubertin, M.R. Julien, S. Servant, D.E. Gill, *Can. Geotech. J.* **36**, 660 (1999).
40. S. Courty, B. Dollet, K. Kassner, A. Renault, F. Graner, *Eur. Phys. J. E* **11**, 5359 (2003).
41. K. Hyun, S.H. Kim, K.H. Ahn, S.J. Lee, *J. Non-Newtonian Fluid Mech.* **107**, 51 (2002).
42. H.G. Sim, K.H. Ahn, S.J. Lee, *J. Non-Newtonian Fluid Mech.* **112**, 237 (2003).
43. T.G. Mason, J. Bibette, D.A. Weitz, *Phys. Rev. Lett.* **75**, 10 (1995).
44. A. Saint-Jalmes, D. Durian, *J. Rheol.* **43**, 6 (1999).
45. F. Da Cruz, F. Chevoir, D. Bonn, P. Coussot, *Phys. Rev. E* **66**, 051305 (2002).
46. P. Coussot, J.S. Raynaud, F. Bertrand, P. Moucheron, J.P. Guilbaud, H.T. Huynh, S. Jarny, D. Lesueur, *Phys. Rev. Lett.* **88**, 218301 (2002).
47. S. Marze, PhD Thesis, Université Paris Sud (2006).
48. J.C. Simo, T.J.R. Hughes, *Computational Inelasticity* (Springer, 1998).
49. F. Elias, C. Flament, J.A. Glazier, F. Graner, Y. Jiang, *Philos. Mag. B* **79**, 729 (1999).
50. P. Jop, Y. Forterre, O. Pouliquen, *Nature* **441**, 727 (2006).
51. C. Raufaste *et al.*, in preparation.
52. B. Dollet, F. Graner, *J. Fluid Mech.* **585**, 181 (2007).
53. L. Berthier, G. Biroli, J.-P. Bouchaud, L. Cipelletti, D.E. Masri, D. L'Hôte, F. Ladieu, M. Pierno, *Science* **310**, 1797 (2005).